Proceedings of *RAGtime 10–13, 15–17/20–22/15–17/14–16 September, 2008/2009/2010/2011, Opava, Czech Republic*
Z. Stuchlík, G. Török and T. Pecháček, editors, Silesian University in Opava, 2014, pp. 1–14

Magnetized tori around Kerr superspinars

Karel Adámek[a] and Zdeněk Stuchlík

Institute of Physics, Faculty of Philosophy & Science, Silesian University in Opava,
Bezručovo nám. 13, CZ-746 01 Opava, Czech Republic
[a]karel.adamek@fpf.slu.cz

ABSTRACT
We study properties of the magnetized toroidal structures orbiting the Kerr superspinars predicted by the string theory. We demonstrate specific features of the unmagnetized perfect fluid tori created in the deep potential well near the surface of the superspinars, enabling clear distinction between Kerr superspinars and black holes. Then we consider the effect of the magnetization of the perfect fluid tori and shift of their properties induced by the presence of the magnetic field.

Keywords: Kerr spacetime – naked singularity – superspinars – magnetized tori

1 INTRODUCTION

Kerr superspinars are considered as primordial, large remnants of very early evolution period of the Universe giving thus signature of the string theory effects (Gimon and Hořava, 2009). However it cannot be excluded that Kerr superspinars were created by the collapse of superspinning differentially rotating compact stars (Giacomazzo et al., 2011). The superspinars are not contradicting the Penrose cosmic censorship hypothesis (Penrose, 1969) since their extension is expected to be limited to $r < R < M$ covering thus the region of causality violations by a correctly behaving stringy solution. Outside a Kerr superspinar, the standard Kerr naked singularity geometry is assumed.

Unstable gravitational perturbation modes has been found for Kerr superspinars with small values of the spin (Pani et al., 2010), however, it does not prove a general instability of Kerr superspinars, since mixing of modes, accretion phenomena or change of boundary conditions related to the Universe expansion could alter the conclusion on the instability. Although there is no uniqueness theorem for Kerr naked singularities (superspinars) similar to the one holding for Kerr black holes, studies of astrophysical phenomena in Kerr naked singularity (superspinars) backgrounds could be quite relevant and useful at least as a test bed model for more complex objects (D. and Manko, 1991). It is convenient (and standardly applied in the literature) to assume the surface radius of Kerr superspinars at $r(\theta) = R = 0.1\,M$, here we shall use the minimal restriction of $R = 0$.

Kerr superspinars (or Kerr naked singularities) were extensively studied for a variety of astrophysical (de Felice, 1974; Calvani and Nobili, 1979; Stuchlík, 1980; Gibbons and Hawking, 1977) and optical (Stuchlík, 1981; Stuchlík and Hledík, 2000; Stuchlík and

978-80-7510-125-9

Schee, 2010, 2011) phenomena. Considering evolution of primordial Kerr superspinars due to Keplerian accretion discs, it has been demonstrated that they could well survive to the era of high-redshift quasars or even longer, if the amount of accreting matter is limited (Stuchlík et al., 2011). Of course it is of high relevance to consider the properties of thick accretion discs represented by toroidal structures of perfect fluid that are complementary to Keplerian thin discs. Here we shall discuss such tori including even the effect of a magnetic field on their structure assuming for simplicity tori with uniform distribution of the specific angular momentum.

2 KERR SUPERSPINARS

In the Boyer–Lindquist coordinates and the geometrical units, the exterior of Kerr superspinars is governed by the line element (Kerr, 1963; Misner et al., 1973)

$$\mathrm{d}s^2 = -\left(1 - \frac{2Mr}{\Sigma}\right)\mathrm{d}t^2 + \frac{\Sigma}{\Delta}\,\mathrm{d}r^2 + \Sigma\,\mathrm{d}\theta^2 + \frac{A}{\Sigma}\sin^2\theta\,\mathrm{d}\varphi^2 - \frac{4M^2ar\sin^2\theta}{\Sigma}\,\mathrm{d}t\,\mathrm{d}\varphi\,, \quad (1)$$

where

$$\Delta = r^2 - 2Mr + \big(aM\big)^2\,, \quad \Sigma = r^2 + \big(aM\big)^2\cos^2\theta\,, \quad (2)$$

and

$$A = \Big(r^2 + \big(aM\big)^2\Big)^2 - \Delta\big(aM\big)^2\sin^2\theta\,, \quad (3)$$

M is mass and $a > 1$ is dimensionless spin of the superspinar.

The physical ring singularity of the spacetime is located at $r = 0, \theta = \pi/2$. The causality violation region is determined by Carter (1973)

$$g_{\phi\phi} = \left[r^2 + (aM)^2 + \frac{2M^3a^2r\sin^2\theta}{\Sigma}\right]\sin^2\theta < 0\,; \quad (4)$$

it can occur only at $r < 0$ (Calvani et al., 1978). Realistic models of Kerr superspinars have to remove the causality violating region and the ring singularity. Therefore, the minimal condition for the boundary surface of Kerr superspinars reads $r(\theta) = R = 0$. In recent papers concerning the Kerr superspinars, the boundary at $r(\theta) = R = 0.1\,M$ is assumed (Gimon and Hořava, 2009; Takahashi and Takahashi, 2010; Pani et al., 2010; Stuchlík and Schee, 2010). We keep this assumption, guaranteeing that all the interesting physical phenomena could be relevant (Stuchlík, 1980; Stuchlík et al., 2011).

The geodesic motion in the Kerr spacetimes is given in a separated and integrated form by the Carter (1973):

$$\Sigma\dot{r} = \pm\sqrt{R(r)}\,, \quad (5)$$

$$\Sigma\dot{\theta} = \pm\sqrt{W(\theta)}\,, \quad (6)$$

$$\Sigma\dot{\phi} = -\left(aE - \frac{\Phi}{\sin^2\theta}\right) + \frac{a}{\Delta}P(r)\,, \quad (7)$$

$$\Sigma\dot{t} = -a\big(aE\sin^2\theta - \Phi\big) + \frac{r^2 + a^2}{\Delta}P(r)\,, \quad (8)$$

where $\dot{} \equiv \mathrm{d}/\mathrm{d}w$ with w being the affine parameter and

$$P(r) = E\left(r^2 + a^2\right) - \Phi a\,, \tag{9}$$

$$R(r) = P^2 - \Delta\left[m^2 r^2 + (\Phi - aE)^2 + Q\right], \tag{10}$$

$$W(\theta) = Q - \cos^2\theta\left[a^2\left(m^2 - E^2\right) + \frac{\Phi^2}{\sin^2\theta}\right]. \tag{11}$$

The motion constants are energy relative to infinity E, angular momentum about the symmetry axis Φ, rest mass m and Q related to the total angular momentum (Carter, 1973). For equatorial motion $Q = 0$. The radial profiles of the specific energy E_{K}/m and specific axial angular momentum Φ_{K}/m of the equatorial circular geodesics are given by Bardeen et al. (1972) and Stuchlík (1980):

$$\frac{E_{\mathrm{K}}}{m} = \frac{r^{3/2} - 2r^{1/2} \pm a}{r^{3/4}\sqrt{r^{3/2} - 3r^{1/2} \pm 2a}}\,, \tag{12}$$

$$\frac{\Phi_{\mathrm{K}}}{mM} = \pm\frac{r^2 + a^2 \mp 2ar^{1/2}}{r^{3/4}\sqrt{r^{3/2} - 3r^{1/2} \pm 2a}}\,, \tag{13}$$

where we introduced dimensionless radial coordinate $r/M \to r$.

The Keplerian velocity with respect to static observers at infinity $\Omega = \mathrm{d}\phi/\mathrm{d}t$ is given by the relation

$$\Omega_{\mathrm{K}} = \pm\frac{1}{M\left(r^{3/2} \pm a\right)} \tag{14}$$

and the profile of the specific angular momentum related to the covariant energy is given by

$$l_{\mathrm{K}} = \frac{\Phi_{\mathrm{K}}}{E_{\mathrm{K}}} = \pm\frac{r^2 \mp 2ar^{1/2} + a^2}{r^{3/2} - 2r^{1/2} \pm a}\,. \tag{15}$$

Behaviour of $l_{\mathrm{K}}(r; a)$ is crucial for determining of the equilibrium tori since it determines the centre and cusps of the tori. The upper (lower) sign in these and the following relations corresponds to the circular geodesics of the 1st (2nd) family. All the 2nd family orbits are counterrotating with $\Phi/mM < 0$. The 1st family orbits are co-rotating ($\Phi/mM > 0$) everywhere in the field of superspinars with spin $a > a_{\mathrm{c}} = 3^{3/2}/4 \sim 1.3$, but they are counter-rotating, with $\Phi/mM < 0$, if appropriately located in the vicinity of superspinars with spin $a < a_{\mathrm{c}}$. Clearly, the 1st family orbits can extend down to the superspinar, they are allowed at all $r > 0$. On the other hand, the 2nd family orbits are allowed at $r > r_{\mathrm{ph}}$; the retrograde photon circular orbit has radius given by

$$r_{\mathrm{ph}} = 2 + \left[a + \sqrt{a^2 - 1}\right]^{2/3} + \left[a + \sqrt{a^2 - 1}\right]^{-2/3}. \tag{16}$$

The limit value for extreme black holes is $r_{\mathrm{ph}}(a = 1) = 4$. The bound orbits (with $E/m < 1$) that could be relevant in toroidal discs (Kozlowski et al., 1978; Stuchlík et al.,

2000; Slaný and Stuchlík, 2005) are limited by the radii of marginally bound orbits with $E/m = 1$ given by

$$r_{\rm mb} = 2 + a \pm 2(1+a)^{1/2}\,, \tag{17}$$

There is $r_{\rm mb}(a = 1) = 5.38$ for the 2nd family orbits and $r_{\rm mb}(a = 1) = 0.172$ for the 1st family orbits. The stable circular orbits determining the inner edge of the Keplerian discs are allowed at radii $r > r_{\rm ms}$; the innermost (marginally) stable circular orbit (ISCO) is determined by

$$r_{\rm ms} = 3 + Z_2 \mp \sqrt{(3 - Z_2)(3 + Z_1 + 2Z_2)}\,, \tag{18}$$

where

$$Z_1 = 1 + \left(1 - a^2\right)^{1/3}\left[(1+a)^{1/3}(1-a)^{1/3}\right], \quad Z_2 = \sqrt{3a^2 + Z_1^2}\,. \tag{19}$$

The minimal value of $r_{\rm ms} = 2M/3$ is obtained for superspinars with $a = a_{\rm e} = (4/3)(2/3)^{1/2} \sim 1.089$ (Stuchlík, 1980). On the other hand, $r_{\rm ms} \to M$ from below when $a \to 1$ from above. Notice that the Kerr superspinar surface radius $r(\theta) = R = 0.1\,M$ is really chosen in such a way that the inner edge of both thin ($r_{\rm in} = r_{\rm ms}$) and thick ($r_{\rm ms} > r_{\rm in} > r_{\rm mb}$) accretion discs is located above the surface.

The 1st family orbits are co-rotating relative to distant observers ($\Omega_{\rm K} > 0$) – such orbits are locally co-rotating ($\Phi_{\rm K} > 0$) in regions distant from superspinars, but could be locally counter-rotating ($\Phi_{\rm K} < 0$) in vicinity of superspinars with the spin parameter $a < a_{\rm c} = (3/4)\,3^{1/2} \sim 1.3$. For superspinars with spin $a < a_{\rm e} = (3/4)\,(3/2)^{1/2} \sim 1.089$ the 1st family orbits with $\Phi_{\rm K} < 0$ could have negative energy ($E < 0$), while located close enough to the superspinar boundary. The marginally stable circular orbit of 1st family is located under $x = 1$ for $a < 5/3$ (Stuchlík, 1980).

The 1st family orbits reveal a strong jump in their properties when transition from a naked singularity spacetime to a black hole spacetime occurs. The jump is most profoundly demonstrated for the profiles of near-extreme Kerr superspinar and Kerr black hole states with spin $a = 1 \pm \delta, \delta \ll 1$ – in the Kerr superspinar spacetimes, stable circular orbits exist at $x = 1$ for all $\delta > 0$, while in the Kerr black hole spacetimes, the stable circular orbits exist at $x > 1$ for $\delta > 0$ and there is an enormous jump between the energy level of the ISCO orbits in the superspinar and black hole spacetimes. On the other hand, the 2nd family orbits are counter-rotating relative to distant observers ($\Omega_{\rm K} < 0$) and locally counter-rotating ($\Phi_{\rm K} < 0$) at all $r > r_{\rm ph}$ for all Kerr superspinars. The Keplerian energy $E_{\rm K}$ and angular momentum $\Phi_{\rm K}$ radial profiles of 2nd family orbits change smoothly when the conversion from the superspinar to the black hole state with $a = 1$ occurs (Stuchlík et al., 2011).

3 MAGNETIZED PERFECT FLUID TORI

Properties of the radial profiles of Keplerian specific angular momentum $l_{\rm K}(r; a)$ are crucial for governing accretion toroidal structures of perfect fluid since the centre of the tori and its cusp, i.e. the edge of accretion tori, are given by condition $l(r) = l_{\rm K}(r)$, where $l(r)$

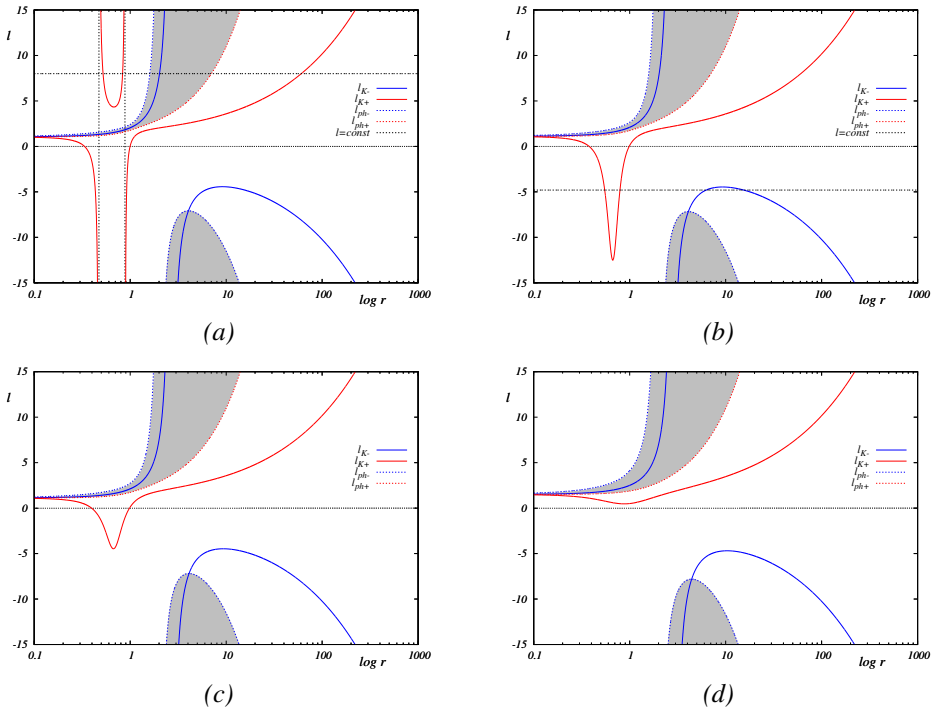

Figure 1. Behaviour of Keplerian angular momentum $l_{\mathrm{K}+}$ and $l_{\mathrm{K}-}$ for *(a)* $a = 1.05$, *(b)* $a = 1.1$, *(c)* $a = 1.118$ and *(d)* $a = 1.5$. The inner disc configurations are possible in the cases *(a)* and *(b)*, for the case *(c)* and *(d)* the inner disc configuration are not possible. For specific angular momentum $l > l_{\mathrm{min}}$ in the case *(a)* and for $l_{\mathrm{min}+} < l < l_{\mathrm{max}-}$ in the case *(b)* it is possible to have both inner and outer discs for the same $l = \mathrm{const}$. As examples we have used two values of the specific angular momentum l, in the case *(a)* it is $l = 8.0$ and in the case *(b)* it is $l = -4.8$. Both $l = \mathrm{const}$ are show as dotted horizontal lines. Regions without circular orbits are greyed out.

is the profile of the angular momentum distribution in the equatorial plane of the tori. Profiles of $l_{\mathrm{K}}(r; a)$ are fundamentally different for Kerr black holes and naked singularities (superspinars), implying fundamental differences of the orbital equilibrium configurations. Here we give overview for superspinars with boundary surface at minimal surface radius $R = 0$ guaranteeing covering of the physical singularity and causality violating region by some regular, say stringy, solution.

We can separate three basic cases of behaviour of the 1st family orbits due to behaviour of $\Phi_{\mathrm{K}}(r; a)$ and $E_{\mathrm{K}}(r; a)$, which can be seen in the Fig. 1. In the field of Kerr superspinars there is no 1st family Keplerian photon circular orbit and the related divergence of l_{K}. However for superspinars with $a < a_{\mathrm{e}} = 1.089$, there is a discontinuity of $l_{\mathrm{K}}(r; a)$ at two radii where $E_{\mathrm{K}}(r; a) = 0$. For $a < a_{\mathrm{c}} \sim 1.3$, $l_{\mathrm{K}}(r; a)$ of 1st family orbits reaches the region of $L < 0$. Then we can obtain possibility to have two distinct tori with the same $l = \mathrm{const} < 0$, if $l_{\mathrm{K}+(\mathrm{min})} < l_{\mathrm{K}-(\mathrm{max})}$. We can demonstrate that this condition can be fulfilled for $a = 1.1 < a_{\mathrm{c}}$.

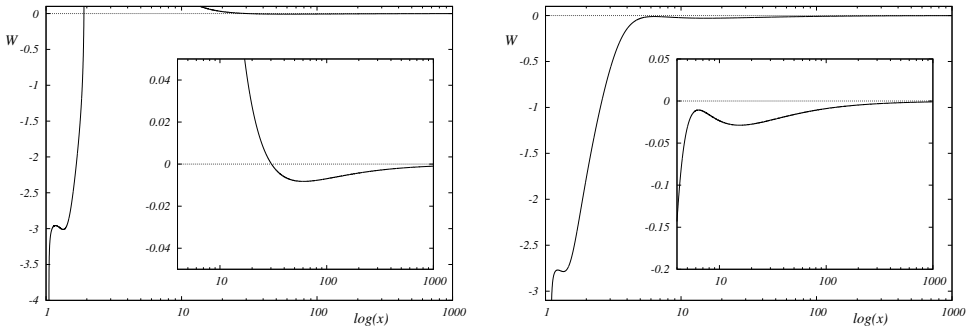

Figure 2. Profiles of the potential W in Kerr–Schild coordinates for $a = 1.05$, $l = 8.0$ in the case *(a)* and for $a = 1.1$, $l = -4.8$ in the case *(b)*.

Rotating perfect fluid is governed by the Boyer's conditions, which implies that boundary of any stationary, barotropic, perfect fluid equilibrium configuration has to be an closed equipotential surface (Boyer, 1965). Equations of the ideal relativistic magnetohydrodynamics (RMHD) of the perfect fluid are for fluid described by stress-energy tensor $T^{\mu\nu}$ and electromagnetic tensor $F^{\mu\nu}$ given by relations (Komissarov, 2006):

$$\nabla_\mu T^{\mu\nu} = 0\,, \tag{20}$$

$$\nabla_\mu {}^*F^{\mu\nu} = 0\,, \tag{21}$$

$$\nabla_\mu F^{\mu\nu} = J^\nu\,, \tag{22}$$

$$\nabla_\mu \rho u^\mu = 0\,. \tag{23}$$

The 4-current J^ν from Maxwell Eq. (22) can be expressed as

$$J^\nu = \sigma e^\nu + q_0 u^\nu\,, \tag{24}$$

where σ is an scalar electric conductivity, q_0 is a electric proper charge and e^ν is 4-vector of the electric field, which in comoving frame reads $e^\nu = (0, \mathbf{E})$, where $\mathbf{E}$ is the 3-vector of the electric field. In the comoving frame and in the kinetic theory approach (Blackman and Field, 1993)

$$J^\nu = \sigma E^j\,. \tag{25}$$

Taking into account the limit of ideal RMHD, $\sigma \to \infty$, and the condition that 4-current must be finite, we get

$$F_{\mu\nu} u^\nu = 0\,. \tag{26}$$

Since $F_{\mu\nu}$ can be fully expressed by the means of b_ν, the Eq. (22) just defines 4-current and it is redundant.

The energy-momentum tensor for ideal perfectly conducting fluid reads

$$T^{\mu\nu} = \left(\omega + b^2\right)u^\mu u^\nu + \left(p + \frac{1}{2}b^2\right) g^{\mu\nu} - b^\mu b^\nu \tag{27}$$

while the Faraday tensor

$${}^*F^{\mu\nu} = b^\mu u^\nu - b^\nu u^\mu \,, \tag{28}$$

where ω, p and u^μ are fluid enthalpy, pressure and 4-velocity respectively, $g_{\mu\nu}$ is the metric tensor and b^μ is the 4-vector of the magnetic field. In the comoving frame $b^\mu = (0, \mathbf{B})$, where $\mathbf{B}$ is 3-vector of the magnetic field measured in comoving frame, thus

$$u^\mu b_\mu = 0 \,. \tag{29}$$

We assume that

- the flow is stationary and axisymmetric; therefore

  $$\partial_t f = \partial_\phi f = 0 \tag{30}$$

  holds for any physical parameter f,
- the flow rotates only

  $$u^r = u^\theta = 0 \,, \tag{31}$$

- the magnetic field is purely azimuthal:

  $$b^r = b^\theta = 0 \,. \tag{32}$$

Under these assumptions the Faraday Eq. (21) and the continuity Eq. (23) are automatically fulfilled and the only non-trivial result follows from projection of the conservation law of the energy-momentum tensor (20) on the hyperplane orthogonal to 4-velocity by the projection tensor $h^\alpha_\beta = \gamma^\alpha_\beta + u^\alpha u_\beta$. From (20) we obtain

$$\left(\omega + b^2\right)u^\nu u_{\nu,i} + \left(p + b^2\right)_{,i} - b_\nu b^\nu_{,i} = 0 \,, \tag{33}$$

where $i = r, \theta$. The angular velocity and specific angular momentum of the rotating fluid are defined by

$$\Omega = \frac{u^\phi}{u^t} \,, \quad l = -\frac{u_\phi}{u_t} \,, \tag{34}$$

implying the relation

$$\Omega = -\frac{l g_{tt} + g_{t\phi}}{l g_{t\phi} + g_{\phi\phi}} \,. \tag{35}$$

Using Eq. (34) we can rewrite Eq. (33) to a form

$$\left(\ln |u_t|\right)_{,i} - \frac{\Omega}{1 - l\Omega} l_{,i} + \frac{p_{,i}}{\omega} + \frac{\left(\mathcal{L}b^2\right)_{,i}}{2\mathcal{L}\omega} = 0 \,, \tag{36}$$

where

$$\left(u_t\right)^2 = \frac{g_{t\phi}^2 - g_{tt}g_{\phi\phi}}{g_{tt}l^2 + 2g_{t\phi}l + g_{\phi\phi}}. \tag{37}$$

Assuming relationship (35), we obtain

$$\mathrm{d}\left(\ln|u_t| + \int_0^p \frac{\mathrm{d}p}{\omega} - \int_0^l \frac{\Omega\,\mathrm{d}l}{1-l\Omega}\right) = -\frac{\mathrm{d}\left(\mathcal{L}b^2\right)}{2\mathcal{L}\omega}\,, \tag{38}$$

where the term in parenthesis is just what we would get for perfect barotropic fluid without magnetic field in it. Following Komissarov (2006) we assume the relationship

$$\tilde{\omega} = \tilde{\omega}(\tilde{p}_{\mathrm{m}})\,, \tag{39}$$

where $\tilde{\omega} = \mathcal{L}\omega$, $\tilde{p}_{\mathrm{m}} = \mathcal{L}p_{\mathrm{m}}$ and $p_{\mathrm{m}} = b^2/2$. Implementing (39) into (38) gives

$$\ln|u_t| + \int_0^p \frac{\mathrm{d}p}{\omega} - \int_0^l \frac{\Omega\,\mathrm{d}l}{1-l\Omega} + \int_0^{p_{\mathrm{m}}} \frac{\mathrm{d}\tilde{p}_{\mathrm{m}}}{\tilde{\omega}} = \mathrm{const}\,. \tag{40}$$

Introducing the total potential W by

$$W = \ln|u_t| + \int_l^{l_\infty} \frac{\Omega\,\mathrm{d}l}{1-l\Omega}\,, \tag{41}$$

where l_∞ is the angular momentum at infinity; assuming that l_∞ is finite, we obtain $u_t(r\to\infty) = -1$ and $W = 0$. Using total potential we arrive at the relation

$$W - W_{\mathrm{in}} + \int_0^p \frac{\mathrm{d}p}{\omega} + \int_0^{p_{\mathrm{m}}} \frac{\mathrm{d}\tilde{p}_{\mathrm{m}}}{\tilde{\omega}} = 0, \tag{42}$$

where W_{in} is the value of the total potential at the inner edge of the disc.

4 CONSTRUCTION OF MAGNETIZED TORI

The simplest configuration occurs if the ideal barotropic fluid has uniform distribution of the specific angular momentum

$$l = l_0 = \mathrm{const}\,. \tag{43}$$

Then the potential governing the equilibrium tori is given by

$$W = \ln|u_t| \tag{44}$$

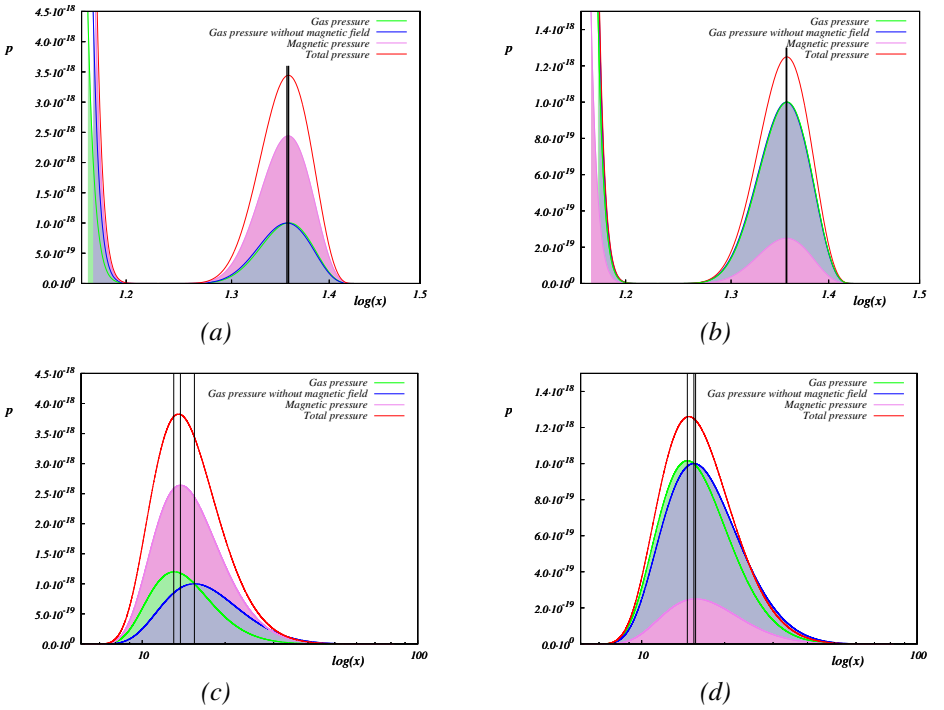

Figure 3. Pressure profiles in Kerr–Schild coordinates for inner discs *(a)*, *(b)* and outer disc *(c)*, *(d)*. with initial magnetization *(a)*, *(c)* $\beta_{\rm c} = 2.5$ and *(b)*, *(d)* $\beta_{\rm c} = 0.25$ for parameters $a = 1.1$, $l_{\rm ms-} > l = -4.8 > l_{\rm mb-}$. The pressure of the gas at the center of the disc is set to $p = 10^{-18}$.

and for $l = \text{const}$ it is given by geometry of the spacetime only. The shape of the equipotential toroidal configurations is illustrated in the Figs. 4 or 5. Following Komissarov (2006) we adopt the these relationships for pressure p and magnetic pressure $p_{\rm m}$

$$p = K\omega^{\kappa}\,, \tag{45}$$

$$p_{\rm m} = K_{\rm m}\mathcal{L}^{\eta-1}\omega^{\eta}\,. \tag{46}$$

Then we can rewrite Eq. (42) into the form

$$W - W_{\rm in} + \frac{\kappa}{\kappa-1}\frac{p}{\omega} + \frac{\eta}{\eta-1}\frac{p_{\rm m}}{\omega} = 0\,. \tag{47}$$

The geometry of the disc is defined by the potential W and the disc center and cusp are defined as points where specific angular momentum of the disc coincides with the specific angular momentum of a particle on the geodetical circular orbit, i.e. where

$$l_0 = l_{\rm K\pm} = \frac{\pm\left(r^2 \mp 2ar^{1/2} + a^2\right)}{r^{3/2} - 2r^{1/2} \pm a}\,; \tag{48}$$

the upper sign holds for co-rotating 1st family orbits while the lower sign holds for counter-rotating 2nd family orbits. Parameters of the model are κ, η, l_0 and $W_{\rm in}$, further parameters are enthalpy at the center of the disc $\omega_{\rm c}$ and initial magnetization

$$\beta_{\rm c} = p_{\rm mc}/p_{\rm c}. \tag{49}$$

From Equation (47) we can separate pressure at the center

$$p_{\rm c} = \omega_{\rm c}\,(W_{\rm in} - W)\left(\frac{\kappa}{\kappa - 1} + \frac{\eta\beta_{\rm c}}{\eta - 1}\right)^{-1}. \tag{50}$$

Using these we can calculate K and $K_{\rm m}$, then separating enthalpy ω from (47) we can get the solution anywhere inside the toroidal disc configuration. We shall focus our attention to the most interesting case when two toroidal configurations with $l = l_0 = \text{const}$ can exist.

4.1 Equilibrium configurations of perfect barotropic fluid

Behaviour of the Keplerian angular momentum $l_{\rm K+}$ and $l_{\rm K-}$ is shown in the Fig. 1. The profiles of the potential W (44) are shown in the Fig. 2. Behaviour of the function $l_{\rm K+}$ strongly depends on the spin parameter a. For $a < a_{\rm e} < 1.089$, a discontinuity occurs due to the fact that circular geodesics with $E_{\rm K} = 0$ exist in such spacetimes. Then the inner configurations with $l = l_0 > 0$ correspond to tori with $\phi = \text{const} < 0$ that are co-rotating relativity to distant observers.

For Kerr naked-singularity metric with rotational parameter $a > 1$, there are two possible disc structures with $l = l_0 = \text{const}$, inner and outer disc. For the 1st family of orbits both inner and outer disc structures are admitted. The inner disc configuration is possible for both $l > 0, a < a_{\rm c}$ and $l < 0, a > a_{\rm c}$ while outer disc configurations can be found only for $l > 0$. Also the inner discs with $l = l_0 < 0$ around naked singularities with $a > a_{\rm c}$ are co-rotating relative to distant observers. The 2nd family admit the outer toroidal configurations only centred around counter-rotating geodesics. We shall concentrate our attention on the case when two equilibrium tori with $l_0 = \text{const}$ are given. We shall study both the inner and outer tori and we are using Kerr–Schild coordinates

$$x = \sqrt{r^2 + a^2}\,\sin\theta\cos\varphi\,, \tag{51}$$

$$y = \sqrt{r^2 + a^2}\,\sin\theta\sin\varphi\,, \tag{52}$$

$$z = r\cos\theta\,, \tag{53}$$

where $y = 0$ due to axial-symmetry.

4.2 Behaviour of the pressure extremes

We are interested in behaviour of gas pressure p, magnetic pressure $p_{\rm m}$ and total pressure $p_{\rm t} = p + p_{\rm m}$ radial profiles and particularly in possible shift of the extreme positions with comparison to the case of a perfect barotropic fluid without magnetic field. We study the difference

$$\Delta x = x^{(a)}_{\rm i(o)} - x_{\rm c}\,, \tag{54}$$

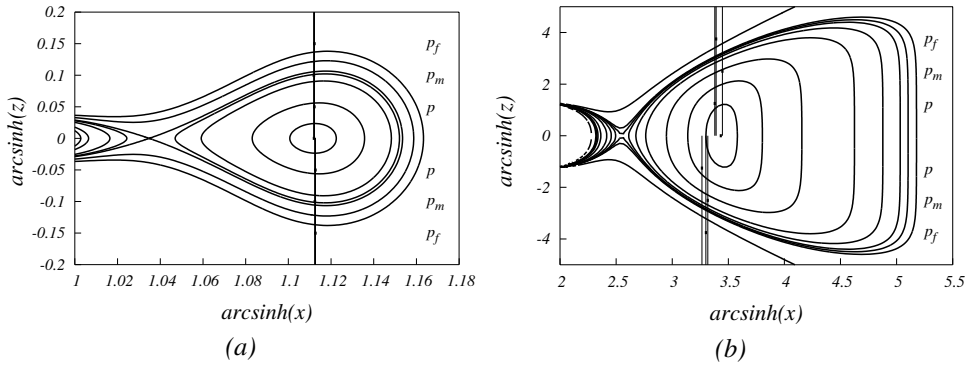

Figure 4. Equipotential surfaces for inner *(a)* and outer *(b)* disc configuration with parameters $a = 1.1$ and $l = -4.8$. Each graph shows two sets of vertical lines, which represent the positions of respective maximums of p, $p_{\rm m}$ and p_f. The upper lines are for initial magnetization $\beta_{\rm c} = 0.25$ while the lower ones are for $\beta_{\rm c} = 2.5$.

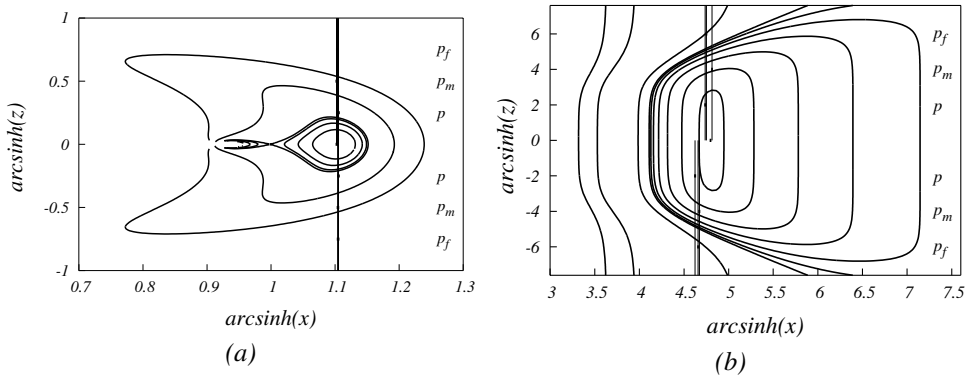

Figure 5. Equipotential surfaces for inner *(a)* and outer *(b)* disc configuration with parameters $a = 1.05$ and $l = 8.0$. Each graph shows two sets of vertical lines, which represent the positions of respective maximums of p, $p_{\rm m}$ and p_f. The upper lines are for initial magnetization $\beta_{\rm c} = 0.25$ while the lower ones are for $\beta_{\rm c} = 2.5$.

where $a = f, m$; $x^{(a)}_{i(o)}$ denotes position of the pressure maximum of fluid (f) and magnetic field (m) for inner (i) and outer (o) discs. Pressure profiles for inner disc configurations and outer disc configurations are shown in the Fig. 3. For outer disc configurations we can see that maximum of the total pressure is shifted closer to a compact object. For inner discs the maximum of the total pressure is receding from the compact object. This behaviour is consistent for all investigated inner and outer disc configurations. Numerical calculations of extremes of the total pressure are shown in the Figs. 6 and 7.

If the initial magnetization goes to zero ($\beta_{\rm c} \to 0$) the configuration is reduced to the case without magnetic field. If $\beta_{\rm c} \to \infty$ the disc is dominated by the magnetic pressure, while gas pressure vanishes. In this case the maximum of magnetic pressure reaches its maximal deviation, this is in the Figs. 6 and 7 depicted as a vertical line.

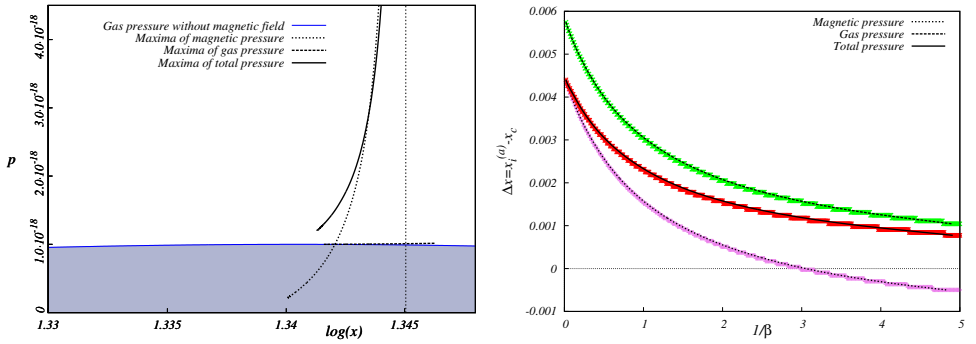

Figure 6. Behaviour of the maximum's position $x_{\mathrm{i}}^{(a)}$ and it's distance $\Delta x = x_{\mathrm{i}}^{(a)} - x_{\mathrm{e}}$ from the disc center x_{c} as a function of the initial magnetization β_{c} for inner toroidal disc configurations with parameters set to $a = 1.05$, $l = 8.0$. On the upper graph we can see the positions of the maximum of the pressure for p, p_{m} and p_f compared with the behaviour of the gas pressure without magnetic field (filled area). On the lower graph we can see the distance Δx of the maximum from the disc center x_{c}.

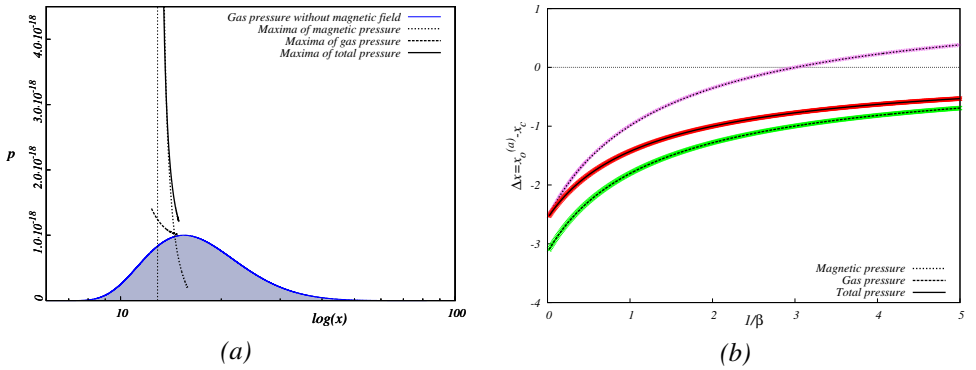

Figure 7. Behaviour of the maximum's position $x_{\mathrm{i}}^{(a)}$ and it's distance $\Delta x = x_{\mathrm{i}}^{(a)} - x_{\mathrm{e}}$ from the disc center x_{c} as a function of the initial magnetization β_{c} for outer toroidal disc configurations with parameters set to $a = 1.1$, $l = -4.8$. On the upper graph we can see the positions of the maximum of the pressure for p, p_{m} and p_f compared with the behaviour of the gas pressure without magnetic field (filled area). On the lower graph we can see the distance Δx of the maximum from the disc center x_{c}.

5 CONCLUSIONS

We have studied magnetized tori around Kerr superspinars, focusing attention to the study of cases when doubled tori exist with the same $l = \mathrm{const}$, and different potential depth. We have demonstrated that the magnetization of the inner tori shifts their pressure maximum away from the Kerr superspinar, while in the outer tori the shift in maximum is toward the Kerr superspinar. We expect this effect could influence the character of optical appearance of oscillating tori around resonant points and we plan to study related phenomena in a future work.

REFERENCES

Bardeen, J. M., Press, W. H. and Teukolsky, S. A. (1972), Rotating black holes: locally nonrotating frames, energy extraction, and scalar synchrotron radiation, *Astrophys. J.*, **178**, pp. 347–369.

Blackman, E. G. and Field, G. B. (1993), Ohm's law for a relativistic pair plasma, *Phys. Rev. Lett.*, **71**, pp. 3481–3484, arXiv: `arXiv:astro-ph/9402068`.

Boyer, R. H. (1965), *Proc. Cambridge Phil. Soc.*, **61**, p. 527.

Calvani, M., de Felice, F., Salmistraro, F. and Muchotrzeb, B. (1978), Time machine and geodesic motion in Kerr metric, *General Relativity and Gravitation*, **9**, pp. 155–163.

Calvani, M. and Nobili, L. (1979), Dressing up a Kerr naked singularity, *Nuovo Cimento B*, **51B**, pp. 247–261.

Carter, B. (1973), Black hole equilibrium states, in C. D. Witt and B. S. D. Witt, editors, *Black Holes*, pp. 57–214, Gordon and Breach, New York–London–Paris.

D., N. I. and Manko, V. S. (1991), On the gravitational field of an arbitrary axisymmetric mass with a magnetic dipole moment, in A. Zichichi, V. de Sabbata and . N. Sanchez, editors, *Gravitation and Modern Cosmology. The Cosmological Constant Problem*, p. 121.

de Felice, F. (1974), Repulsive phenomena and energy emission in the field of a naked singularity, *Astronomy and Astrophysics*, **34**, pp. 15–19, URL `http://adsabs.harvard.edu/article_service.html`.

Giacomazzo, B., Rezzolla, L. and Stergioulas, N. (2011), Collapse of differentially rotating neutron stars and cosmic censorship, *Phys. Rev. D*, **84**, p. 024022 (16 pages), URL `http://link.aps.org/doi/10.1103/PhysRevD.84.024022`.

Gibbons, G. W. and Hawking, S. W. (1977), Cosmological event horizons, thermodynamics, and particle creation, *Phys. Rev. D*, **15**, pp. 2738–2751.

Gimon, E. G. and Hořava, P. (2009), Astrophysical violations of the Kerr bound as a possible signature of string theory, *Phys. Rev. B*, **672**, pp. 299–302, arXiv: `0706.2873`.

Kerr, R. P. (1963), Gravitational Field of a Spinning Mass as an Example of Algebraically Special Metrics, *Phys. Rev. Lett.*, **11**, p. 237.

Komissarov, S. S. (2006), Magnetized tori around Kerr black holes: analytic solutions with a toroidal magnetic field, *Monthly Notices Roy. Astronom. Soc.*, **368**, pp. 993–1000, arXiv: `arXiv:astro-ph/0601678`.

Kozlowski, M., Jaroszyński, M. and Abramowicz, M. A. (1978), The analytic theory of fluid disks orbiting the Kerr black hole, *Astronomy and Astrophysics*, **63**(1–2), pp. 209–220, URL `http://adsabs.harvard.edu/abs/1978A%26A....63..209K`.

Misner, C. W., Thorne, K. S. and Wheeler, J. A. (1973), *Gravitation*, W. H. Freeman and Co, New York, San Francisco.

Pani, P., Barausse, E., Berti, E. and Cardoso, V. (2010), Gravitational instabilities of superspinars, *Phys. Rev. D*, **82**(4), 044009, arXiv: `1006.1863`.

Penrose, R. (1969), Gravitational collapse: The role of general relativity, *Nuovo Cimento B*, **1**(special number), pp. 252–276.

Slaný, P. and Stuchlík, Z. (2005), Relativistic thick discs in the Kerr–de Sitter backgrounds, *Classical Quantum Gravity*, **22**(17), pp. 3623–3651, URL `http://www.iop.org/EJ/abstract/-search=44947255.2/0264-9381/22/17/019`.

Stuchlík, Z. (1980), Equatorial circular orbits and the motion of the shell of dust in the field of a rotating naked singularity, *Bull. Astronom. Inst. Czechoslovakia*, **31**(3), pp. 129–144.

Stuchlík, Z. (1981), Evolution of Kerr naked singularities, *Bull. Astronom. Inst. Czechoslovakia*, **32**(2), pp. 68–72.

Stuchlík, Z. and Hledík, S. (2000), Equatorial photon motion in the Kerr–Newman spacetimes with a non-zero cosmological constant, *Classical Quantum Gravity*, **17**(21), pp. 4541–4576, ISSN 0264-9381/00, arXiv: 0803.2539, URL http://www.iop.org/EJ/abstract/0264-9381/17/21/312.

Stuchlík, Z., Hledík, S. and Truparová, K. (2011), Evolution of Kerr superspinars due to accretion counterrotating thin discs, *Classical Quantum Gravity*, **28**(15), p. 155017.

Stuchlík, Z. and Schee, J. (2010), Appearance of Keplerian discs orbiting Kerr superspinars, *Classical and Quantum Gravity*, **27**(21), p. 215017, arXiv: 1101.3569.

Stuchlík, Z. and Schee, J. (2011), Influence of the cosmological constant on the motion of Magellanic Clouds in the gravitational field of Milky Way, *Journal of Cosmology and Astroparticle Physics*, **9**, p. 18.

Stuchlík, Z., Slaný, P. and Hledík, S. (2000), Equilibrium configurations of perfect fluid orbiting Schwarzschild–de Sitter black holes, *Astronomy and Astrophysics*, **363**(2), pp. 425–439, ISSN 0004-6361 (printed version), 1432-0746 (parallel-to-print version), URL http://adsabs.harvard.edu/abs/2000A%26A...363..425S.

Takahashi, R. and Takahashi, M. (2010), Anisotropic radiation field and trapped photons around the Kerr black hole, *Astronomy and Astrophysics*, **513**, A77, arXiv: 1002.4245.